Journal of Biomechanics 45 (2012) 1379–1386

Contents lists available at SciVerse ScienceDirect

Journal of Biomechanics

journal homepage: www.elsevier.com/locate/jbiomech
www.JBiomech.com

Perturbation-dependent selection of postural feedback gain and its scaling

Seyoung Kim [a], Christopher G. Atkeson [b], Sukyung Park [a,*]

[a] Department of Mechanical Engineering, KAIST, Daejeon, Republic of Korea
[b] Robotics Institute, Carnegie Mellon University, Pittsburgh, PA, USA

ARTICLE INFO

Article history:
Accepted 2 March 2012

Keywords:
Push recovery
Postural control
Feedback gain
Gain scaling
Joint torque

ABSTRACT

In this study we examined whether the selection of postural feedback gain and its scaling is dependent on perturbation type. We compare forward pushes applied to the back of a standing subject to previous work on responses to support translation. As was done in the previous work, we quantified the subject's response in terms of perturbation-dependent feedback gains. Seven healthy young subjects (25 ± 3 yr) experienced five different magnitudes of forward push applied by a 1.25 m-long pendulum falling from the height of 1.4 m toward the center of mass of the subject's torso. The loads on the pendulum ranged from 2 to 10 kg. Impulsive force, ground reaction forces and joint kinematics were measured, and joint torques were calculated from inverse dynamics. A full-state feedback control model was used to quantify the empirical data, and the feedback gains that minimized the fitting error between the data and model simulation were identified. As in previously published feedback gains for support translation trials, gradual gain scaling with push perturbation magnitude was consistently observed, but a different feedback gain set was obtained. The results imply that the nervous system may be aware of body dynamics being subjected to various perturbation types and may select perturbation-dependent postural feedback gains that satisfy postural stability and feasible joint torque constraints.

© 2012 Elsevier Ltd. All rights reserved.

1. Introduction

Postural strategy changes from an ankle strategy to a hip strategy in response to different perturbation magnitudes of support translation (Horak and Nashner, 1986; Runge et al., 1999; Park et al., 2004). Specifically, hip joint torque increases with perturbation, while the increase in the ankle joint torque is more limited due to biomechanical constrains on the maximum allowable ankle joint torque (Runge et al., 1999; Park et al., 2004; Kim et al., 2009). The compensatory joint torques for upright postural balance disturbances have been quantified as having a linear relationship with joint kinematics (Barin, 1989; Speers et al., 1998; Alexandrov et al., 2005) or linear feedback control (Kuo, 1995; Peterka, 2002; Park et al., 2004; Kim et al., 2009). Using a biomechanics model incorporating a feedback controller that reproduces the empirical data, the change of joint kinematics and kinetics with perturbation size was quantified by gradually scaled feedback gains (Park et al., 2004; Kim et al., 2009). For the same magnitude of backward support translation, both healthy young and elderly subjects showed similar feedback gain sets for postural control and gradual gain scaling with perturbation, whereas the age-matched elderly Parkinson patients group showed significantly reduced gain scaling trends, implying that the proposed feedback gain control and its scaling could be a good candidate for quantifying postural strategy change (Kim et al., 2009). The observed postural strategy change quantified by continuous feedback gain scaling, however, would be applicable only to the limited range of postural motion generated by a specific perturbation type, such as backward support translation.

In this paper we investigate whether a different type of perturbation, an impulsive push to the torso, would also be quantifiable by simple feedback control and gain scaling as well as how those gain scaling values would be different from those obtained from the support translation trials. Seven healthy young subjects (25 ± 3 yr) experienced five different magnitudes of a forward push applied by a falling pendulum dropped from the height of 1.4 m toward approximately the center of mass (CoM) of the subject's torso. The loads on the pendulum ranged from 2 to 10 kg. Impulsive force, ground reaction forces, and joint kinematics were measured, and joint torques were calculated from inverse dynamics. A full-state feedback control model was used to quantify the empirical data, and the feedback gains that minimized the fitting error between the data and model simulation were obtained using the optimization toolbox (Matlab®). We then compared the calculated feedback gains and their scaling with perturbation to those from the support translation trials obtained from a previously published study (Park et al., 2004; Kim et al., 2009).

* Correspondence to: Department of Mechanical Engineering, KAIST, 335 Gwahak-ro, Yuseong-gu, Daejeon 305-701, Republic of Korea.
Tel.: +82 42 350 3230; fax: +82 42 350 5230.
E-mail address: sukyungp@kaist.ac.kr (S. Park).

0021-9290/$ - see front matter © 2012 Elsevier Ltd. All rights reserved.
http://dx.doi.org/10.1016/j.jbiomech.2012.03.001

2. Methods

2.1. Experimental procedures

Seven healthy young subjects (M6/W1, mean age: 25 ± 3 yr, mean height: 171 ± 5 cm, mean body mass: 66 ± 4 kg) with no history of balance disorder participated in this study. Before the experiment, all subjects signed consent forms approved by the Institutional Review Board of KAIST. Subjects were instructed to stand upright with their arms crossed over their chest and to recover an upright posture in response to five randomly ordered forward push perturbations of different magnitudes applied by a custom-made hanging pendulum without stepping or lifting their heels, if possible. The magnitude of the push was varied by loading different masses ranging from 2 to 10 kg at the end of the pendulum (Fig. 1A). The pendulum mass and length were 3.8 kg and 1.25 m, respectively, and the length was adjusted slightly to the CoM height of the subject's torso. The pendulum was dropped from a height of 1.4 m toward the back of the subjects when triggered by an electromagnetic switch. The collision velocity of the pendulum was approximately 1.84 m/s. To reduce the back pain at the moment of collision, the subjects wore a sponge-padded backpack. To minimize the anticipation of the onset of pendulum fall, noise was provided to the subjects through a headset. Prior to the data collection, the subjects rehearsed several trials, including the maximum perturbation.

2.2. Measurement

Impulsive force, ground reaction forces, and joint kinematics data were recorded for 10 s, including 2 s of quiet stance prior to the onset of push perturbation. Kinematic data were measured by the Motion Analysis system (4 IR cameras, Motion Analysis Inc., Santa Rosa, California) at a sampling rate of 200 Hz using five reflective markers attached at the shoulder (acromion), hip (greater trochanter), knee (lateral femoral condyle), ankle (lateral malleolus), and the platform surface. Ground reaction forces were recorded by a force plate (AMTI dual force plate) at a sampling rate of 200 Hz, and impulsive force was measured by a load cell (SCM-500 kgf, SENSTECH Inc.) attached at the end of the pendulum at a sampling rate of 1000 Hz.

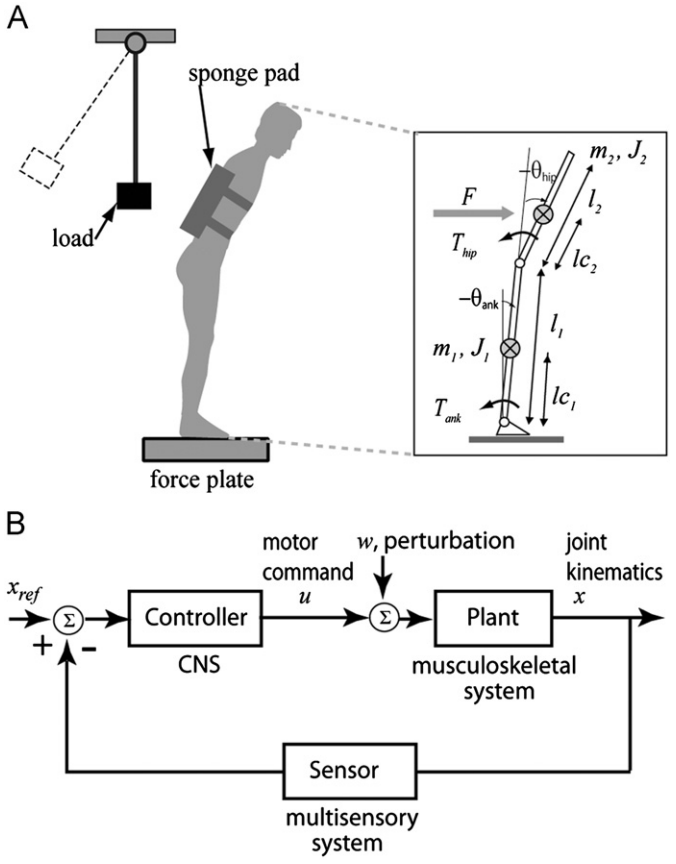

Fig. 1. (A) Schematics of the experimental setup. The subjects initially stood straight up. The pendulum has a mass of 3.8 kg and a length of 1.25 m and was located at 35° referenced to a vertical axis. Five different magnitudes of push impulse were applied by the falling pendulum from a height of 1.4 m with masses ranging from 2 to 10 kg. To reduce the maximum force delivered to the subject to a manageable range, the subjects wore sponge padding on their backs. Noise was provided to the subjects through a headset because sound from the electromagnet may cause anticipation behavior. The postural control model and its variables are depicted with notations (inset). (B) Block diagram of the postural feedback control model. Plant, sensor, and controller represent the musculoskeletal, sensory, and central nervous system, respectively. A 2-segment biomechanical model and a full-state feedback control model were used for the plant and controller model, and perfect sensory dynamics with unity gain was assumed.

2.3. Data analysis

The mechanical model used to simulate the postural response to push perturbation consists of a 2-segment inverted pendulum and feedback controller that generates compensatory joint torques (Fig. 1A and B). The equations of motion for an inverted pendulum were derived using the Newton–Euler equation and linearized with respect to the vertical axis:

$$M\begin{bmatrix}\ddot{\theta}_{ank}\\ \ddot{\theta}_{hip}\end{bmatrix} = G\begin{bmatrix}\theta_{ank}\\ \theta_{hip}\end{bmatrix} + \begin{bmatrix}T_{ank}\\ T_{hip}\end{bmatrix} - P$$

$$\text{where} \quad M = \begin{bmatrix} J_1 + m_1 l_{c1}^2 + m_2 l_1^2 + m_2 l_1 l_{c2} + J_2 + m_2 l_1 l_{c2} + m_2 l_{c2}^2 & J_2 + m_2 l_1 l_{c2} + m_2 l_{c2}^2 \\ m_2 l_1 l_{c2} + J_2 + m_2 l_{c2}^2 & J_2 + m_2 l_{c2}^2 \end{bmatrix}$$

$$G = \begin{bmatrix} m_1 g l_{c1} + m_2 g l_1 + m_2 g l_{c2} & m_2 g l_{c2} \\ m_2 g l_{c2} & m_2 g l_{c2} \end{bmatrix}, \quad P = \begin{bmatrix} l_1 + l_{c2} \\ l_{c2} \end{bmatrix} F \tag{1}$$

where m is the mass, l is the segment length, l_c is the distance from the joint to the center of mass, J is the moment of inertia, and θ_{ank} and θ_{hip} are the ankle and hip joint angles, respectively. T_{ank} and T_{hip} are the ankle joint torque and hip joint torque, respectively, and F is the push force. Subscripts '1' and '2' indicate the lower and upper limbs, respectively (Eq. (1), Fig. 1A). The segmental inertial parameters for the models were obtained from anthropometric tables, and the ankle and hip joint torques were calculated using a least squares inverse dynamics method (Kuo, 1998; Park et al., 2004; Kim et al., 2009).

To formulate the feedback control model, we defined the state vector, x, of joint kinematics referenced to the initial upright posture as $x = \begin{bmatrix}\theta_{ank} & \theta_{hip} & \dot{\theta}_{ank} & \dot{\theta}_{hip}\end{bmatrix}^T$, where $\dot{\theta}_{ank}$ and $\dot{\theta}_{hip}$ are the ankle and hip angular velocities, respectively. The state-space equation of the postural control system was obtained, $\dot{x} = Ax + Bu + C$, where A and B are the state matrices obtained in terms of inertial parameters of the body segments and C is the vector of the push perturbation:

$$A = \begin{bmatrix} 0 & 0 & 1 & 0 \\ 0 & 0 & 0 & 1 \\ M^{-1}G & & 0 & 0 \\ & & 0 & 0 \end{bmatrix}, \quad B = \begin{bmatrix} 0 & 0 \\ 0 & 0 \\ M^{-1} & \end{bmatrix}, \quad C = \begin{bmatrix} 0 \\ 0 \\ M^{-1}P \end{bmatrix} \tag{2}$$

Feedback control input u (i.e., joint torque T) was assumed to be generated by full-state feedback in the following form:

$$u \equiv T = -Kx$$

$$\text{where} \quad T = \begin{bmatrix}T_{ank} & T_{hip}\end{bmatrix}^T, \quad K = \begin{bmatrix} k_{11} & k_{12} & k_{13} & k_{14} \\ k_{21} & k_{22} & k_{23} & k_{24} \end{bmatrix},$$

$$x = \begin{bmatrix}\theta_{ank} & \theta_{hip} & \dot{\theta}_{ank} & \dot{\theta}_{hip}\end{bmatrix}^T \tag{3}$$

To quantify the postural response change in terms of feedback gain scaling so that the feedback-controlled system model is then formulated in the form of $\dot{x} = (A - BK)x + C$, where K is the only variable to identify, we solved the differential equation with initial condition x_0 and a push force F obtained from inverse dynamics. Because we performed the dynamic simulation during the period ($\sim$300 ms) before the onset of perturbation, the initial condition was almost zero, but it often deviated slightly from zero for the trials in which the subjects had an initial offset posture from the averaged upright posture. The desired position is upright, and the desired velocity is zero.

The impulsive force applied by the falling pendulum was transmitted to the subject through a sponge-padded backpack. Because it is practically difficult to create and maintain a direct attachment of a force sensor to the back of a subject with a consistent sensor configuration, we indirectly estimated the push force F using inverse dynamics with a least squares penalty that fits both the measured joint kinematics and the ground reaction forces (Fig. 2A; see the details in electronic Supplementary material). Due to the imperfection of the rigid body biomechanics modeling used for inverse dynamics, motion artifacts such as negative push-forces were observed, which however does not significantly change the calculation of the system response. We then used the estimated push perturbation P for the linear system (Eq. (3)) simulation.

To identify the feedback gain that reproduces the perturbed postural responses, we used an optimization that minimizes the data fitting error from model simulation using sequential quadratic programming (fmincon, Matlab®). We excluded the first $\sim$1.5 s of quiet stance from the 10 s of data recorded during each trial and fit the model to the following 5 s of the data (e.g., measured joint

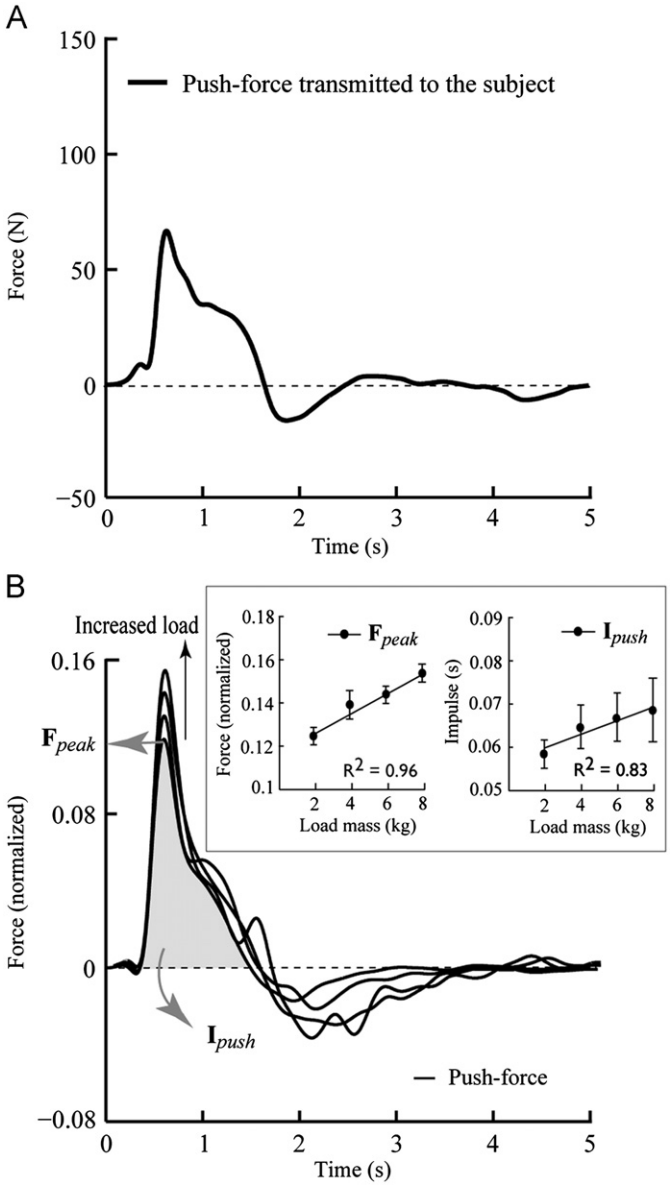

Fig. 2. Push force estimation from inverse dynamics: (A) Representative push-force transmitted to the subject through the sponge padding estimated from inverse dynamics. When an impulsive force from a pendulum fall is applied to the back of the subject through the sponge padding, the magnitude and duration of collision force were significantly changed by additional padded backpack dynamics. (B) Push force estimation from inverse dynamics for various pendulum loads ranging from 2 to 8 kg. The proportionality of the peak force and impulse with respect to the load holds in an almost linear manner (inset). Both force (N) and impulse (N s) were normalized to the body weight (N) of the subject. Error bars indicate standard errors.

motions and torques) because most of the subjects recovered their upright posture within 5 s of the stimulus. Details of the gain identification were presented in previously published papers (Park et al., 2004; Kim et al., 2009). Once we obtained the feedback gain sets that best match the empirical joint kinematics and kinetics data, the change of gain parameters as a function of perturbation magnitude was statistically tested using regression analysis with the level of significance as $p<0.05$. It is important to note that the obtained feedback gain K is the static map between control (u) and state (x) in the form of $u=-Kx$, should not be directly interpreted as a closed-loop system parameter identification, which requires multiple perturbations for unique identification.

To examine the kinetic and kinematic changes generated by different feedback gain selections for push perturbation, as opposed to the previously derived feedback gains used for support translations (Park et al., 2004; Kim et al., 2009), model simulations of joint motion and torques using two gain sets for push and support translation in response to both perturbation types were compared with each other (Figs. 6 and 7). Specifically, we tested whether the identified feedback gain sets were applicable to other types of perturbation in view of postural stability and feasible joint torque constraints by examining the time response of joint angles and torques for two different gain sets (Fig. 6) as well as the maximum excursion of joint angles and torques to a broader range of feedback gains and perturbation magnitudes (Fig. 7). Maximum values of perturbed response were simulated using postural feedback gain sets identified from small to large push (2–8 kg load) and support translation (3–12 cm for 275 ms) perturbation trials in response to small to large push (Fig. 7A–D) and support translation perturbations (Fig. 7E–H). Initial condition and reference values for the simulation were set to quiet upright posture, i.e., zero values, and the disturbance inputs for simulation were obtained from the empirical push and support translation stimulus profiles shown in Fig. 6B and D with the onset time of 300 ms. The state-space equations (Eq. (2)) were then solved using an ordinary differential equation solver (lsim, Matlab®), and the simulations were recorded for 5 s, including 300 ms of upright posture prior to the onset of each perturbation. To simulate postural response for backward support translation, the perturbation matrix of Eq. (1) was replaced by

$$P=-\begin{bmatrix} m_1lc_1+m_2l_1+m_2lc_2 \\ m_2lc_2 \end{bmatrix}a,$$

where a is the platform acceleration obtained empirically from the platform encoder (Park et al., 2004; Kim et al., 2009). The body parameters used for simulation were obtained from the average values for all participating subjects.

3. Results

Most subjects successfully recovered their upright posture without violation of the flat-foot constraints for most of the perturbations, except the largest perturbation, which was designed to induce either heel-off or stepping. One subject showed frequent heel-offs or steps, even to the smallest push perturbation, and his data were not included in the analysis.

When impulsive force by pendulum fall is applied to the back of the subject through the sponge padding, the magnitude and duration of the collision force were significantly changed by the additional padded backpack dynamics (Fig. 2A). Although the padded backpack significantly changed the impulsive force distribution, the proportionality of the peak force and impulse with respect to the mass of falling loads ranging from 2 to 8 kg follows an almost linear trend (Fig. 2B). Joint torques and angles increased with push and showed non-uniform scaling (Fig. 3). Although ankle joint motion was smaller compared to hip joint motion (Fig. 3B), relatively similar ankle joint torque was generated (Fig. 3A). Specifically, even for the smallest push, the subjects generated ankle torques up to the amount of 0.08 (normalized torque by subject's weight multiplied by height, approximately 80 N m), which is close to the maximum allowable ankle joint torque (approximately 100–125 N m). Note that the ankle joint torque seemed to reach its maximum allowable limit even for the second smallest push magnitude, while hip joint torque proportionally increased with push amplitude (Fig. 3A). Push perturbations applied approximately to the torso CoM mostly generate hip response, i.e., out-of-phase motion between the upper and lower extremities (Fig. 3B).

A linear feedback control model reproduced the data for all subjects with an average goodness of fit of $R^2=0.83\pm0.04$ (Fig. 4). Multiple gain components of the feedback gain, K in Eq. (3), showed gradual scaling with push magnitude (Fig. 5, Table 1). An increase of feedback gain generally indicates greater contribution of the corresponding kinematic deviation to the generation of compensatory joint torque. Most feedback gain parameters (k_{11}, k_{12}, k_{13}, k_{22}, k_{23}, and k_{24}) showed a statistically significant decreasing trend with perturbation magnitude ($p<0.05$). Ankle torque-related gains (k_{12}, k_{13}, k_{14}) for push were comparatively larger, whereas hip torque-related gains (k_{21}, k_{22}, k_{24}) were smaller than those for support translation. Although dominant hip strategy engagement was observed due to the difference in perturbation type, the changes of postural strategy from the ankle to the hip were consistently observed for both tasks, which were quantified as scaled feedback gains.

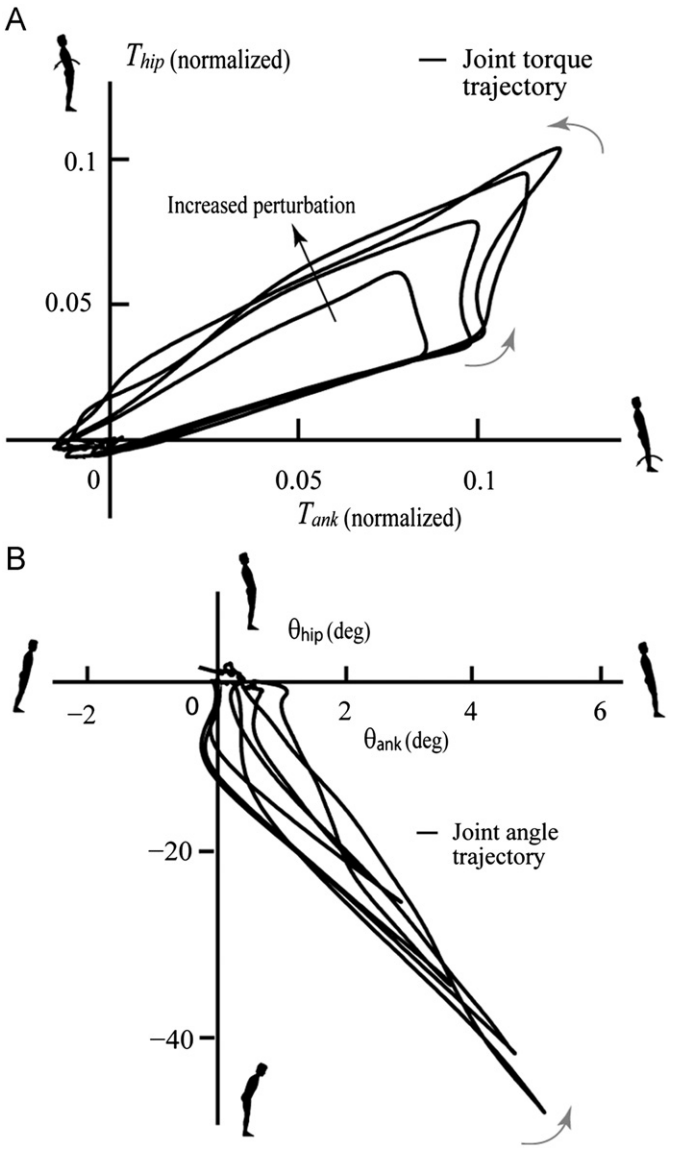

Fig. 3. Joint kinematics and kinetics data: (A) Averaged joint torque and (B) joint angle trajectories of all subjects for various push magnitudes. Joint torque (N m) was normalized by each subject's weight (N) multiplied by height (m). Joint angles (deg.) were defined from subjects' initial upright posture with a positive sign for extension in the sagittal plane. Non-uniform scaling of joint torques and angles with push perturbation was observed. The *x*- and *y*-axis use different scales for better visibility.

Model predictions demonstrate that perturbation specific gain selection facilitates postural control, subject to perturbation-dependent biomechanical constraints (Figs. 6 and 7). For example, compared with the support translation trials, push perturbation applied to the upper extremity induces hip joint excursion and the deviation of the center of mass in a more direct manner. Therefore, to maintain balance in response to a large hip joint excursion due to a push stimulus while not violating the flat-foot constraint, ankle joint motion was significantly restricted compared with the response obtained from the support translation gains (Fig. 6B). The stiffened ankle joint caused by larger ankle feedback push gains (Fig. 5) makes the hip joint relatively flexible. When a support translation stimulus was applied for push gain-controlled body dynamics, the relatively flexible hip joint induced greater hip joint motion compared with the model simulation with support translation gains (Fig. 6D). Greater ankle feedback push gains (Fig. 5) also resulted in stiffened body posture and faster joint motion and actuation torque compared with the translation gain simulation in response to the same perturbation (Fig. 6).

Model simulation also demonstrates that perturbation-dependent gain selection results in more restricted joint kinetics than joint kinematics. For two different gain selections, a large difference in the joint excursion of up to an order of magnitude was observed (Fig. 6B and D); however, this did not necessarily induce a similar order of magnitude of joint torque difference (Fig. 6A and C).

To examine whether the previously observed response change with different gain selections is observed consistently for a broader range of perturbation, the model simulation was extended to the various perturbation magnitude and gain selection combinations (Fig. 7). Greatly restrained ankle response by greater push gains were consistently observed for various push sizes and gains (Fig. 7A–D). Large push gains induce stiffened ankle joints and relatively flexible hip joints, which results in greater hip joint excursions being consistently observed for various perturbation magnitudes (Fig. 7D) and types (Fig. 7F and H). The effect of different gain selections was highlighted for greater postural challenges, such as push trials and trials with greater perturbation magnitude and feedback gains identified for large perturbations, because greater postural challenges require more conservative postural control action to maintain balance. It has clearly been shown that a smaller peak ankle but larger peak hip joint angles are required for the gains from push trials to maintain balance during the stabilizing process over a wide range of perturbations (Fig. 7C, D, G, and H). Therefore, the difference in postural response could be summarized as greater engagement of hip joint motion with restrained ankle joint motion for the push recovery process. Suppressed ankle joint motion for push trials was simulated by using a similar magnitude of the ankle angle feedback (k_{11}) and

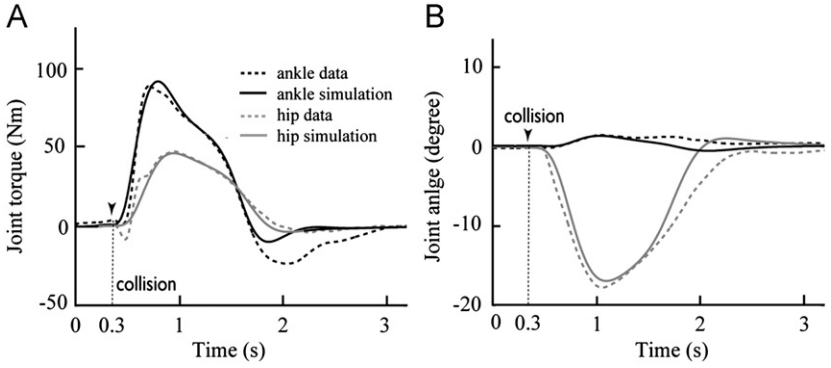

Fig. 4. A representative data-fitting result: (A) Joint torque and (B) joint angle data (dotted lines) for a 6 kg load mass were fitted by a 2-segment inverted pendulum model simulation (solid lines). The onset of push perturbation occurred at approximately $t=0.3$ s (inverse triangle). Ankle and hip joint responses are differentiated by the black and gray colors, respectively. The R^2 value obtained from comparing the data with the simulations was 0.88.

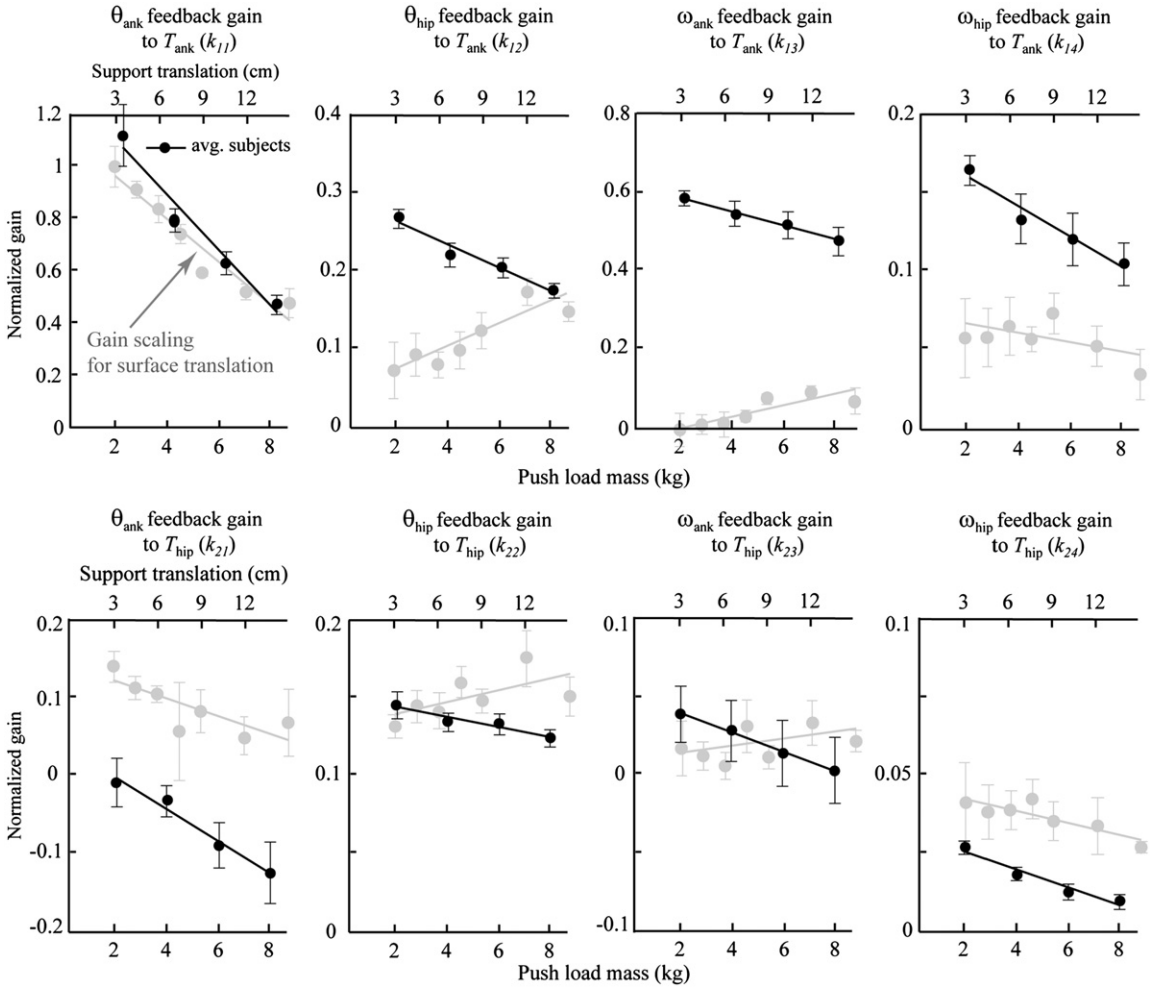

Fig. 5. Averaged feedback gain components for all subjects (filled circle) obtained from the model that minimizes the data-fitting error. Gradual gain scaling values with push magnitude and linear regressions (black solid lines) were all statistically significant ($p < 0.05$). Error bars indicate standard errors. Position gains (k_{11}, k_{12}, k_{21}, k_{22}) were normalized to the product of the subject's weight (N) and height (m), and differential gains (k_{13}, k_{14}, k_{23}, k_{24}) were normalized to the product of subject's weight (N), height (m), and the square root of the subject's height (m) divided by the gravitational acceleration (m/s^2). Previously published gain parameters for support translation trials (Kim et al., 2009) are displayed together (gray) for comparison.

Table 1
Linear regression coefficients for scaled feedback gains of all subjects.

Gain	Linear regression	
	Slope	Intercept
k_{11}	-0.097 ± 0.043	1.231 ± 0.281
k_{12}	-0.016 ± 0.003	0.303 ± 0.036
k_{13}	-0.022 ± 0.020	0.658 ± 0.072
k_{14}	-0.012 ± 0.003	0.197 ± 0.018
k_{21}	-0.017 ± 0.017	0.008 ± 0.091
k_{22}	-0.004 ± 0.003	0.155 ± 0.025
k_{23}	-0.006 ± 0.003	0.053 ± 0.067
k_{24}	-0.003 ± 0.001	0.032 ± 0.003

larger hip feedback gains (k_{12} and k_{14}) (Fig. 5), which generated faster oscillatory ankle joint kinematics (Fig. 6B and D). Greater ankle torque-related gains (k_{12}, k_{13}, and k_{14}) for push trials also contributed to the reduced ankle joint torque generation (Fig. 6A).

4. Discussion

In this study, we quantified the perturbation-dependent change of the postural strategy using feedback gain scaling. A linear feedback control model and its gain scaling with the push perturbation magnitude quantified the relationship between the joint torques and kinematics during push-recovery reasonably well (Figs. 4 and 5), similar to the previous attempts applied to support-surface translation trials (Park et al., 2004; Kim et al., 2009). To examine the appropriateness of perturbation-dependent gain selection, we compared the simulation results of double inverted pendulum dynamics with various feedback gain sets that were obtained from push and support translation trials (Figs. 6 and 7). The result of undesirable joint excursions by inappropriate gain selection (Fig. 7) implies that the nervous system may be aware of body dynamics and biomechanical constraints and selects appropriate postural feedback gains that satisfy postural stability and feasible joint torque constraints. Consistent with the support translation trials (Park et al., 2004; Kim et al., 2009), most gains gradually scaled with the perturbation magnitude (Fig. 5) to accommodate the maximum allowable ankle torque constraint (Fig. 3A). The decrease in ankle torque-related gains (k_{11}, k_{12}, k_{13}, k_{14}) with increasing perturbation (Fig. 5) demonstrates that the ankle joint motion was not compensated for as severely as it was for the trials that had a larger gain, mostly due to the feasible ankle torque constraint.

Because the feedback control model was used to quantify the change of empirical data of postural responses, its role was descriptive rather than predictive. The relationship between the

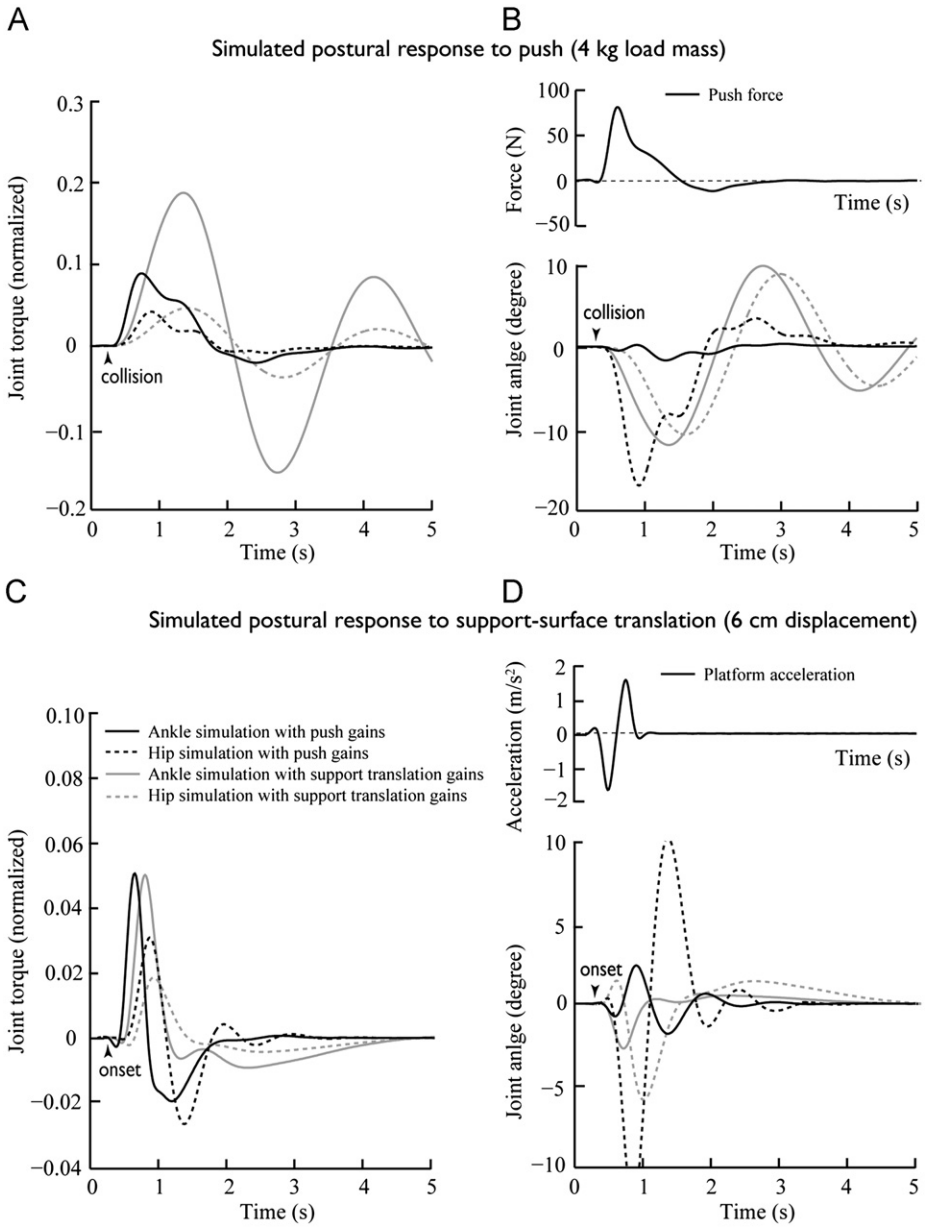

Fig. 6. A model prediction of postural response using a 2-segment inverted pendulum controlled by two different gains selected from push (black) and support translation (gray) trials, respectively. Simulated joint kinetics and kinematics for push stimulus (A, B), and support-surface translation (C, D) applied at the time $t \approx 0.3$ s. Corresponding push and support translation stimulus are presented in the right panel (B, D). Ankle and hip joint responses are shown as solid and dashed lines, respectively. Joint torques of the ankle and hip were normalized for the subject's weight multiplied by height. In response to the same perturbation, different feedback gains demonstrate significantly different joint kinematics and kinetics.

change of joint kinematics and kinetics and gain scaling, however, may suggest a possible control objective for a predictive postural control model. The gradual suppression of the increase of ankle torque observed for both perturbation trials (Fig. 7A and E) implies that the maximum allowable ankle torque constraint needs to be implemented for the postural control objective in a continuous manner, such as in the form of a soft constraint (Park, 2002; Park et al., 2004; Kim et al., 2009). Gain scaling with perturbation occurs in such a way as to reduce the excessive joint torque generation (Fig. 7A, E and F), whereas the joint angle deviation was not severely restricted (Fig. 7D and G), which is consistent with previous attempts to create an optimal control model that penalizes excessive joint torque and postural deviation from upright to represent postural responses (Kuo, 1995; Atkeson and Stephens, 2008). Therefore, one may suggest a control objective for postural feedback control that minimizes the joint torque actuation as well as the joint kinematics with the continuous enforcement of biomechanical constraints.

It is worth noting that the reasonable match between the model and the data should be interpreted as a successful attempt to quantify the postural strategy change in terms of feedback gain scaling, but not as an explicit demonstration of the postural feedback control mechanism by the nervous system. The quantification of postural response change using feedback gains and their scaling is mathematically equivalent to the system response from dynamic parameter changes, such as stiffness and the damping coefficient. Specifically, when a simple mass (m)–damper (c) system written as $m\ddot{x}+c\dot{x}=0$ is controlled by a proportional position controller with a gain K_p that exerts a displacement proportional restoring control force as follows, $m\ddot{x}+c\dot{x}=-K_Px$, then it is physically equivalent to the attachment of a spring component with stiffness K_s. The equation of motion for this case also has a similar form: $m\ddot{x}+c\dot{x}+K_sx=0$. Similarly, the system

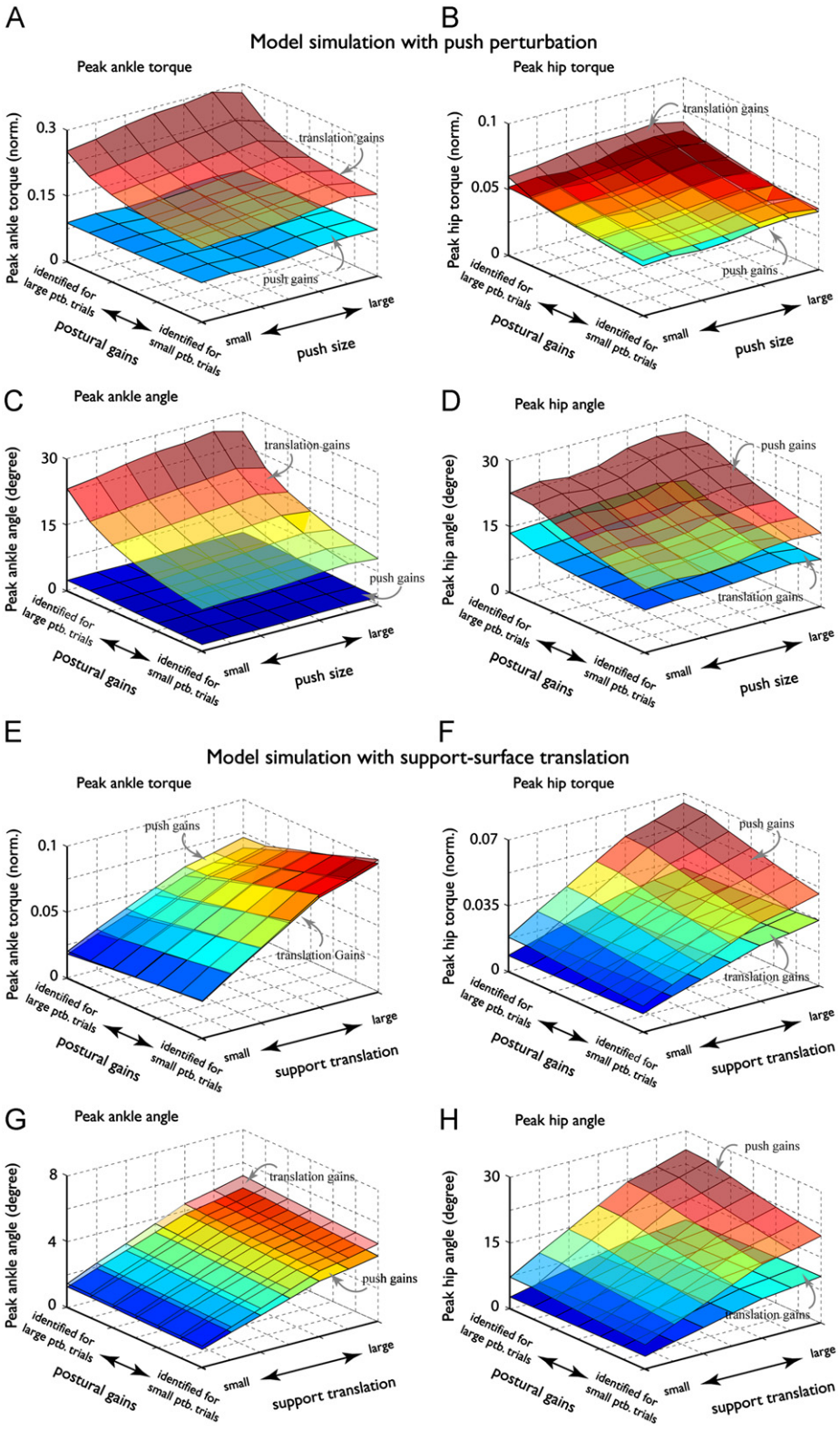

Fig. 7. Model simulation of peak joint torque and angle with respect to a broader range of feedback gains and perturbation magnitudes. Various postural gain sets identified from data for small to large postural perturbations, i.e., push and support translations, were pooled for simulation. The empirical ranges of various perturbation magnitudes were used for simulation. Peak joint torques (A, B) and angles (C, D) for push perturbations are shown on the top panels, and those for support translations are shown on the bottom (E–H). The average body weight and height of all subjects were used for the simulation. The peak joint torques of the ankle and hip were normalized to the subject's weight multiplied by height.

parameter identification from the single response would not differentiate the existence of a feedback controller or the dynamics-driven response. Therefore, the observed non-uniform scaling of joint kinematics and kinetics with perturbation could be attributed to either a change of system dynamics parameters or feedback control gain scaling. Based on previous reports from the control perspective of postural control and the change of postural strategy observed from perturbation recovery (Peterka, 2000; Morasso and Sanguineti, 2002;

Kuo, 2005; Goodworth and Peterka, 2010), in this study, we interpreted the postural strategy change as feedback gain scaling, which again does not exclude the possibility of the contribution of joint dynamics changes.

Conflict of interest statement

None.

Acknowledgments

This research was supported by the Basic Science Research Program through the National Research Foundation of Korea (NRF) funded by the Ministry of Education, Science and Technology (#2010-0013306), the Happy tech. program through the National Research Foundation of Korea (NRF) funded by the Ministry of Education, Science and Technology (#2010-0020488), the US National Science Foundation under Grants EEC-0540865, ECCS-0824077, and IIS-0964581 and the DARPA M3 program. The authors thank Jin Yeom, Myunghyun Lee and Changwon Lee for their contributions to data collection.

Appendix A. Supplementary material

Supplementary data associated with this article can be found in the online version at http://dx.doi.org/10.1016/j.jbiomech.2012.03.001.

References

Alexandrov, A., Frolov, A., Horak, F., Carlson-Kuhta, P., Park, S., 2005. Feedback equilibrium control during human standing. Biological Cybernetics 93, 309–322.

Atkeson, C.G., Stephens, B., 2008. Multiple balance strategies from one optimization criterion. In: Proceedings of the 2007 7th IEEE-RAS International Conference on Humanoid Robots. HUMANOIDS 2007. Pittsburgh, PA, pp. 57–64.

Barin, K., 1989. Evaluation of a generalized model of human postural dynamics and control in the sagittal plane. Biological Cybernetics 61, 37–50.

Goodworth, A.D., Peterka, R.J., 2010. Influence of stance width on frontal plane postural dynamics and coordination in human balance control. Journal of Neurophysiology 104, 1103–1118.

Horak, F.B., Nashner, L.M., 1986. Central programming of postural movements: adaptation to altered support-surface configurations. Journal of Neurophysiology 55, 1369–1381.

Kim, S., Horak, F.B., Carlson-Kuhta, P., Park, S., 2009. Postural feedback scaling deficits in Parkinson's disease. Journal of Neurophysiology 102, 2910–2920.

Kuo, A.D., 1995. An optimal control model for analyzing human postural balance. IEEE Transactions on Biomedical Engineering 42, 87–101.

Kuo, A.D., 1998. A least-squares estimation approach to improving the precision of inverse dynamics computations. Journal of Biomechanical Engineering 120, 148–159.

Kuo, A.D., 2005. An optimal state estimation model of sensory integration in human postural balance. Journal of Neural Engineering 2, S235–S249.

Morasso, P.G., Sanguineti, V., 2002. Ankle muscle stiffness alone cannot stabilize balance during quiet standing. Journal of Neurophysiology 88, 2157–2162.

Park, S., 2002. Human Standing Postural Control Adjusts to Biomechanical Constraints. Ph.D. Thesis. University of Michigan, Ann Arbor.

Park, S., Horak, F.B., Kuo, A.D., 2004. Postural feedback responses scale with biomechanical constraints in human standing. Experimental Brain Research 154, 417–427.

Peterka, R.J., 2000. Postural control model interpretation of stabilogram diffusion analysis. Biological Cybernetics 82, 335–343.

Peterka, R.J., 2002. Sensorimotor integration in human postural control. Journal of Neurophysiology 88, 1097–1118.

Runge, C.F., Shupert, C.L., Horak, F.B., Zajac, F.E., 1999. Ankle and hip postural strategies defined by joint torques. Gait and Posture 10, 161–170.

Speers, R.A., Paloski, W.H., Kuo, A.D., 1998. Multivariate changes in coordination of postural control following spaceflight. Journal of Biomechanics 31, 883–889.